JOINT INSTITUTE FOR NUCLEAR RESEARCH
Veksler and Baldin Laboratory of High Energy Physics

FINAL REPORT ON THE START PROGRAMME

Ξ AND Ω RECONSTRUCTION IN AU+AU COLLISIONS AT $\sqrt{s_{NN}} = 27$ GEV WITH THE STAR EXPERIMENT

Student:
Artem Timofeev, Russia
Moscow State University

Supervisor:
Ph.D. Alexey A. Aparin

Participation period:
July 01 - August 24

Dubna
2024

Abstract

A large amount of experimental data has been collected in the Beam Energy Scan program to study the properties of hot matter formed in heavy-ion collisions. This work presents the reconstruction and analysis of multi-strange particles, specifically $\Xi^{-}(\bar{\Xi}^{+})$ and $\Omega^{-}(\bar{\Omega}^{+})$, produced in Au+Au collisions at $\sqrt{s_{NN}} = 27$ GeV using data from the *STAR* experiment at the RHIC accelerator. The study focuses on the identification of these particles through their decay channels and the subsequent analysis of their invariant mass distributions and transverse momentum spectra.

Contents

1 Introduction

Quantum Chromodynamics (QCD) is the theory of the strong interaction in terms of quarks and gluons. The main properties of the strong interaction are:

- confinement, which prohibits quarks and gluons from existing in a free state;
- asymptotic freedom, which is the weakening of the strong interaction constant as the distance between interacting objects decreases.

At high densities of hadronic matter or at high temperatures, quarks are no longer confined and can move freely within a volume larger than that of an individual hadron. This state is called deconfinement, and the state of matter is referred to as quark-gluon plasma (QGP). Such conditions can be observed at modern high-energy colliders such as *RHIC* and *LHC*, with maximum beam energies in the center of mass system of 200 GeV/A and 6.8 TeV, respectively.

One of the main goals of high-energy physics experiments is the study of the QCD phase diagram, plotted in *Fig. 1*, which is conveniently considered in the coordinates of temperature T and baryochemical potential μ_B. This diagram includes the QGP area, which is of particular interest for the *STAR* experiment at the *RHIC* accelerator. To study hot matter, the *Beam Energy Scan (BES)* program was launched, and its main goals are: 1) to search for a first-order QCD phase transition and determine its parameters; and 2) to determine the energy onset of deconfinement[1].

An increased yield of strange particles in heavy-ion collisions compared to proton collisions has long been considered a signal of QGP formation [2]. The yield of strange hadrons in nuclear collisions is close to theoretical predictions; therefore, their precise measurement will lead to a better understanding of the mechanism of strangeness formation in hot matter, as well as narrowing the search area for freeze-out parameters.

Strange particles are a good marker for identifying phase boundaries and the onset of deconfinement; therefore, the goal of this work is to reconstruct strange particles with the *STAR* experiment at $\sqrt{s_{NN}} = 27$ GeV, as well as to inspect

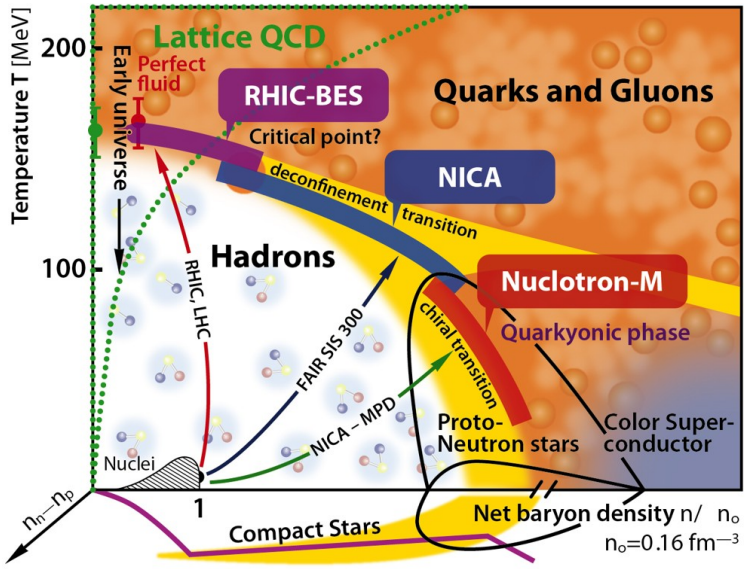

Figure 1: QCD matter phase diagram.

their properties. The study focuses on multi-strange particles such as $\Xi^- \left(\bar{\Xi}^+\right)$ and $\Omega^- \left(\bar{\Omega}^+\right)$. Since the decay length of these particles is $c\tau \sim 2 - 7$ cm, the detector cannot directly register them. In this case, particles are reconstructed from their decay modes, used in this work as follows:

$$\begin{aligned}
\Lambda \left(\bar{\Lambda}\right) &\rightarrow p \left(\bar{p}\right) + \pi^- \left(\pi^+\right), \ BR = 64.1\%; \\
\Xi^- \left(\bar{\Xi}^+\right) &\rightarrow \Lambda \left(\bar{\Lambda}\right) + \pi^- \left(\pi^+\right), \ BR = 99.887\%; \\
\Omega^- \left(\bar{\Omega}^+\right) &\rightarrow \Lambda \left(\bar{\Lambda}\right) + K^- \left(K^+\right), \ BR = 67.8\%.
\end{aligned}$$

2 Experimental Setup

Solenoidal Tracker At RHIC (STAR) is a multipurpose particle detector at the *RHIC* accelerator, located at the Brookhaven National Laboratory. A detailed description of the detector can be found in [3].

Time Projection Chamber (TPC) (shown in Fig. 2) is the main detector at the *STAR* facility. It allows the registration of charged particles in the range $[0, 2\pi]$ of the azimuthal angle, as well as in the range $|\eta| < 1$, where η is the pseudorapidity.

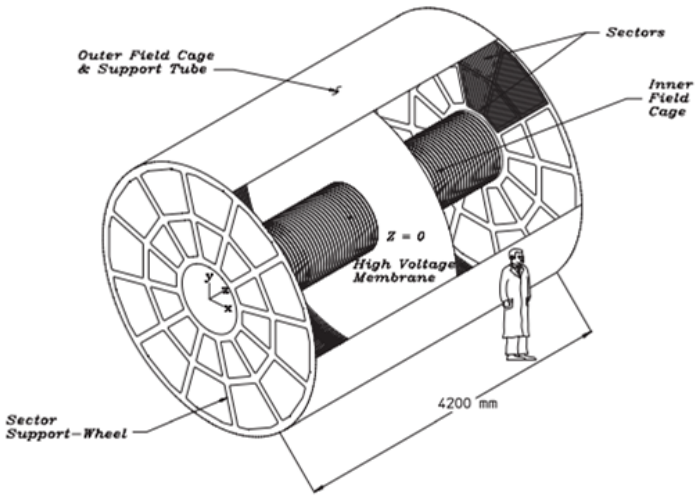

Figure 2: TPC scheme.

Inside the *STAR* detector, a uniform magnetic field is maintained, directed along the beam axis, with an induction of 0.5 Tesla. The *TPC* consists of two coaxial cylinders: the inner radius is 0.5 m, and the outer is 2 m. The space between them is filled with P10 gas in a uniform electric field of approximately 135 V/m. Each track can leave up to 45 hits in the *TPC*, with a minimum transverse momentum of 100 MeV/c. Particle identification is carried out using ionization losses dE/dx by introducing the parameter

$$n\sigma_{particle} = \frac{1}{\sigma_{particle}} \cdot \log \frac{\langle dE/dx \rangle_{measured}}{\langle dE/dx \rangle_{theoretical}},$$

where $\langle dE/dx \rangle_{measured}$ is the measured, and $\langle dE/dx \rangle_{theoretical}$ is the theoretical value for a specific particle at a given momentum; $\sigma_{particle}$ is the detector resolution for measuring ionization losses.

The data used for particle reconstruction are from Au+Au collisions at $\sqrt{s_{NN}} = 27$ GeV from BES-II program. The number of events processed in this work is approximately $877 \cdot 10^6$.

3 Analysis Details

3.1 Event Selection

Since one of the goals of this work is to investigate rapidity dependence of spectra, we must not study events with their position close to detector edges. To achieve that we applied the following cuts on event vertex position: along the Z axis, directed along the beam axis, the event must be located in the range from -70 cm to 70 cm; in the XY plane, perpendicular to the Z axis, closer than 2 cm from the center of the detector. In *Fig.* 3, the events distribution is presented with the selection criteria graphically applied. The selected area ensures the most uniform registration of particles by the detector, the statistical significance of the obtained data, and coverage of the area $|\eta| < 1$. After these selection criteria, approximately $450 \cdot 10^6$ events remain.

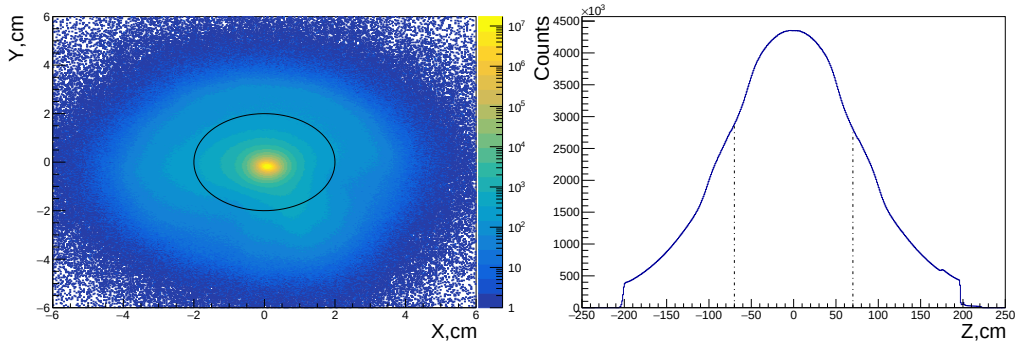

Figure 3: Event coordinate distributions in the XY plane (left) and along the Z axis (right). Black lines represent the selection criteria.

3.2 Secondary track selection

The distribution of ionization losses of charged particles in the *TPC* is close to Gaussian, therefore a selection criterion of $|n\sigma_{particle}| < 4.0$ was applied to all selected daughter particles in this work, and $|n\sigma_{particle}| < 3.0$ for protons for reconstructing Ω. Also, a minimum number of hits that a particle must leave was 16; minimum transverse momentum was 0.1 GeV/c and the $|\eta| < 1$. The energy

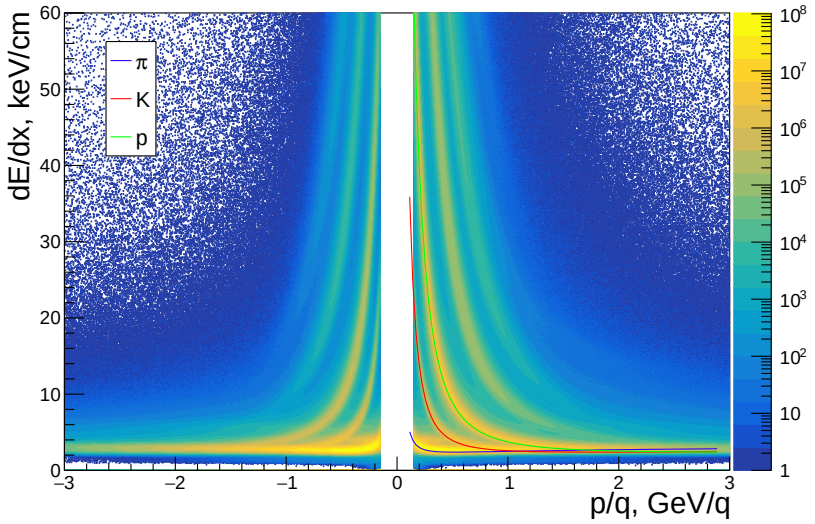

Figure 4: Energy losses $\langle dE/dx \rangle$ for charged particles as a function of rigidity (p/q). Colored lines show the theoretical values for the corresponding particles.

losses for particles registered by *TPC* are presented in *Fig. 4* after applying the above selection criteria, as well as the theoretical dependencies. It is noticeable that separate identification of pions and kaons is not possible in the region $p_T \gtrsim 0.6$ GeV/c, and for protons at $p_T \gtrsim 1.2$ GeV/c.

3.3 Reconstruction of Strange Particles

3.3.1 General Methodology

The reconstruction of strange particles used a combinatorial method (each pair consisting of $p^{\pm}$ and $\pi^{\mp}$ in the case of Λ, and consisting of Λ and $\pi^{\mp}$ $(K^{\mp})$ in the case of Ξ (Ω)) with the StPicoDst library, which allows working with the *STAR* experiment data. The trajectories of charged particles represent helices directed along the beam axis, while uncharged particles correspond to straight lines. Based on this, the main idea of reconstruction was to find the point of closest approach between the trajectories, with the subsequent determination of the decay geometry and kinematic parameters of the particles in this area. In *Fig. 5*, the schemes of Ξ and Ω decay topology are shown.

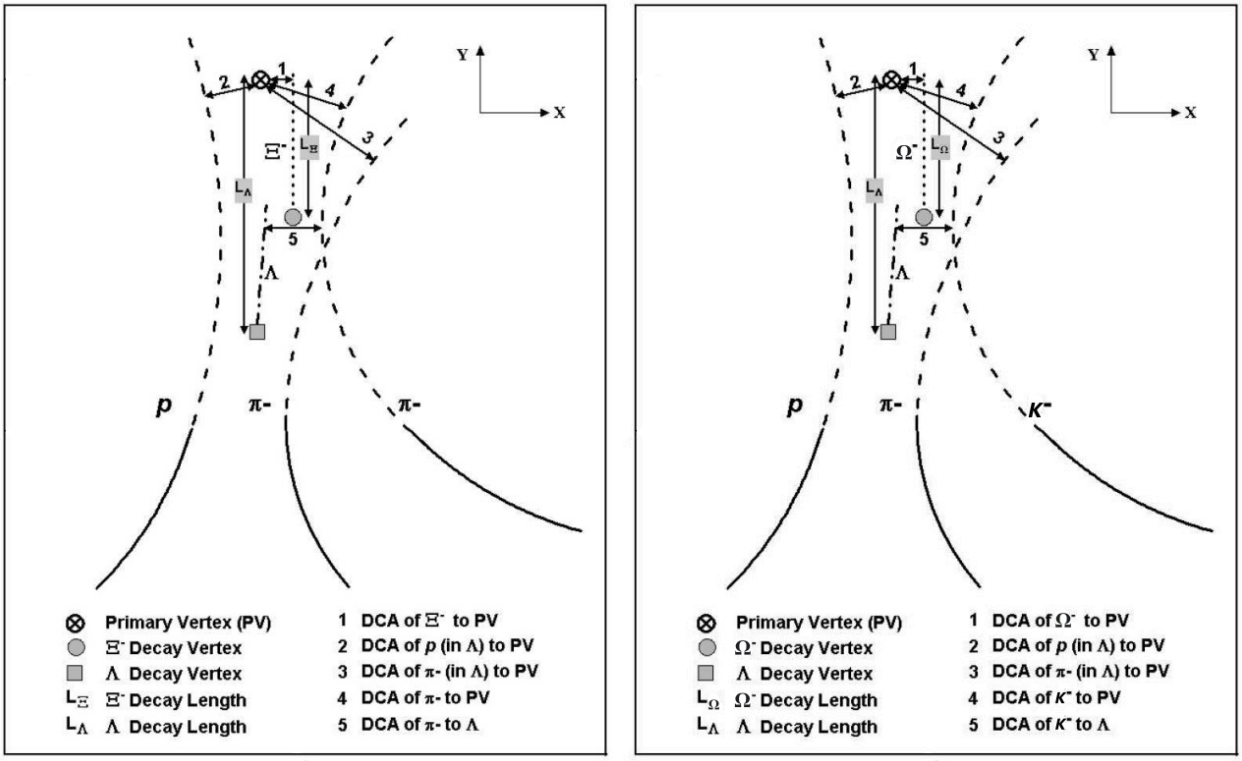

Figure 5: Decay topology of Ξ and Ω. Solid lines are the tracks registered in the TPC, dashed lines are the extrapolation of solid lines. DCA — distance of closest approach, PV — primary event vertex.

As heavy-ion collisions produce a large number of particles, the use of a combinatorial method in the invariant mass distributions for all strange particles introduces a large number of background events, which need to be maximally suppressed. For this purpose, certain selection criteria on the decay topology for Ξ and Ω, presented in *Table* 1 and *Table 2*, were applied. The closer look at decay topology is in *Section 3.3.2* of this work. These criteria provide a balance between signal purity and statistical significance. A selection criterion based on the invariant mass of Λ was also applied — it must be in the range $[M_\Lambda \pm 0.012$ GeV/c$^2]$ for Ξ and $[M_\Lambda \pm 0.006$ GeV/c$^2]$ for Ω.

Besides the combinatorial background, there is also a residual background for each particle due to unavoidable particle misidentification. For example, the bachelor pion from Ξ decay may be misidentified as kaon thereby contributing into Ω signal. Also in Ξ reconstruction, a proton from Λ decay can be combined

with another pion into fake Λ, which when combined with pion from Λ (as bachelor pion) constructing fake Ξ. To avoid it, the following cuts were applied for Ξ reconstruction:

- proton from Λ is combined with bachelor pion. If invariant mass of this pair falls inside Λ peak, the Ξ candidate is rejected;
- bachelor pion is assumed to be a kaon to re-calculate the invaraint mass. If it falls inside Ω peak, candidate is rejected;

and for Ω reconstruction:

- bachelor kaon is assumed to be a pion to re-calculate the invaraint mass. If it falls inside Ξ peak, candidate is rejected.

Table 1: Selection Criteria for Ξ

Cut	$\Xi^-\left(\bar{\Xi}^+\right)$
DCA of Ξ to primary vertex	< 0.8 cm
DCA of π to primary vertex	> 0.8 cm
DCA of Λ to primary vertex	$[0.2, 5.0]$ cm
DCA of p from Λ to primary vertex	> 0.5 cm
DCA of π from Λ to primary vertex	> 1.0 cm
DCA between Λ daughter particles	< 0.8 cm
DCA between Λ and π	< 0.8 cm
Λ decay length	> 5 cm
Ξ decay length	> 3.4 cm
$(\overrightarrow{r}_{\Xi} - \overrightarrow{r}_{PV}) \cdot \overrightarrow{r}_{\Xi}$	> 0
$(\overrightarrow{r}_{\Lambda} - \overrightarrow{r}_{PV}) \cdot \overrightarrow{r}_{\Lambda}$	> 0
$(\overrightarrow{r}_{\Lambda} - \overrightarrow{r}_{\Xi}) \cdot \overrightarrow{r}_{\Lambda}$	> 0
$(\overrightarrow{r}_{\Xi} - \overrightarrow{r}_{PV}) \times \vec{p_{\Xi}} / \left\lvert \vec{r_{\Xi}} - \vec{r_{PV}} \right\rvert / \left\lvert \vec{p_{\Xi}} \right\rvert$	< 0.2

Table 2: Selection Criteria for Ω

Cut	Ω^- $\left(\bar{\Omega}^+\right)$
DCA of Ω to primary vertex	$< 0.4\,(< 0.5)$ cm
DCA of K to primary vertex	> 1.0 cm
DCA of Λ to primary vertex	> 0.4 cm
DCA of p from Λ to primary vertex	> 0.6 cm
DCA of π from Λ to primary vertex	> 2.0 cm
DCA between Λ daughter particles	< 0.7 cm
DCA between Λ and π	< 0.7 cm
Λ decay length	> 3.0 cm
Ω decay length	> 3.4 cm
$(\overrightarrow{r}_{\Omega} - \overrightarrow{r}_{PV}) \cdot \overrightarrow{r}_{\Omega}$	> 0
$(\overrightarrow{r}_{\Lambda} - \overrightarrow{r}_{PV}) \cdot \overrightarrow{r}_{\Lambda}$	> 0
$(\overrightarrow{r}_{\Lambda} - \overrightarrow{r}_{\Omega}) \cdot \overrightarrow{r}_{\Lambda}$	> 0
$(\overrightarrow{r}_{\Omega} - \overrightarrow{r}_{PV}) \times \vec{p_{\Omega}} / \left\lvert \vec{r_{\Omega}} - \vec{r_{PV}} \right\rvert / \left\lvert \vec{p_{\Omega}} \right\rvert$	< 0.12

3.3.2 Search of Decay Point

As mentioned earlier, the trajectories of charged particles represent helices directed along the external magnetic field. In this regard, finding the decay vertex V^0 involves finding the intersection points of two spirals, which is implemented as follows:

- By projecting the trajectories of charged particles onto the XY plane we get circles;
- After we find the intersection points of these circles (usually one of the intersection points is discarded, as the curvature radius of the trajectory significantly exceeds the detector size);
- After all We calculate the 3D coordinates of these points.

Then, the midpoint of the segment connecting the obtained points will be considered as the coordinate of the V^0 decay. If the obtained decay geometry passes all the selection criteria on Λ, listed in *Table 1* and *Table 2*, this candidate is saved for further analysis.

In the case of Ξ and Ω, which decay into V^0 and a charged particle, it is necessary to consider the intersection of the line Δ and the helix C (*see Fig. 6*). The algorithm is almost similar to the search of V^0 decay point. At the point M where trajectories of decay particles intersect in XY plane, the trajectory $\mathcal{C}$ of π/K is linearized. Further the points H_1 and H_2 of the closest approach of these lines are found. The midpoint of the segment H_1H_2 is the decay vertex of Ξ/Ω. If the decay geometry passes the selection criteria presented in *Table 1* and *Table 2*, the candidate is saved as Ξ/Ω. At this point, the invariant mass is calculated as

$$m^2_{\Xi,\Omega} = \left(\sqrt{\overrightarrow{p}^2_{\Lambda} + m^2_{\Lambda}} + \sqrt{\overrightarrow{p}^2_{\pi,K} + m^2_{\pi,K}}\right)^2 - \overrightarrow{p}^2_{\Xi,\Omega},$$

where $\overrightarrow{p}_{\pi,K}$ is the momentum of π/K at point M.

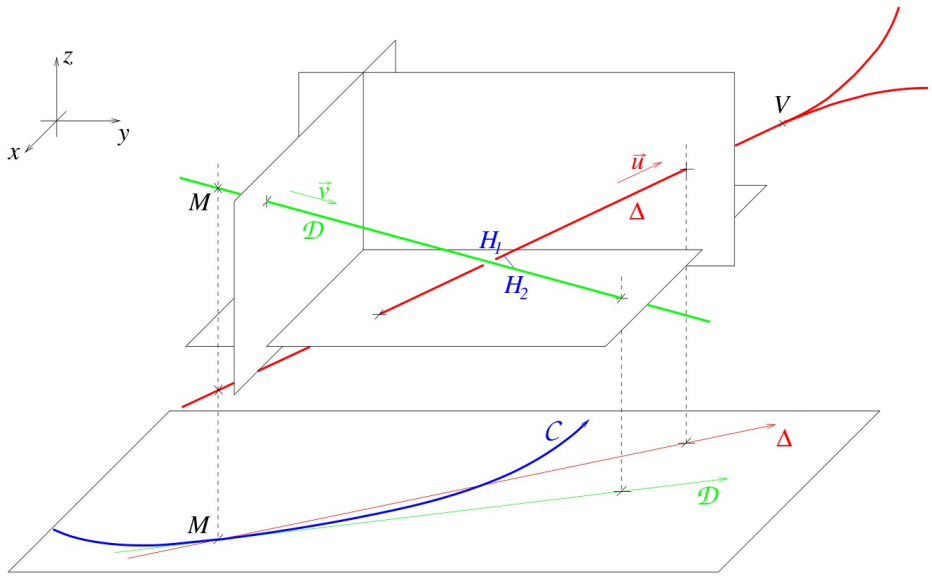

Figure 6: Decay geometry of Ξ/Ω. Point M — the intersection point of $\mathcal{C}$ and Δ. The blue curve represents part of the projection of the trajectory of π/K onto the XY plane, the red line represents the trajectory of V^0, and green is the tangent $\mathcal{D}$ to the trajectory of $\mathcal{C}$ at point M. Point V is the decay vertex of V^0, H_1 and H_2 are the points of closest approach of the lines $\mathcal{D}$ and Δ.

3.3.3 Armenteros-Podolanski Diagram

The reconstruction of particles occurs using information only about their kinematic characteristics. In this case, the Armenteros-Podolanski diagram [4] becomes convenient, as it considers the correlation between the magnitude of the transverse momentum $p_\perp$ and a dimensionless quantity

$$\alpha_{arm} = \frac{p_L^+ - p_L^-}{p_L^+ + p_L^-}, \tag{1}$$

where p_L is the longitudinal momentum in the direction of the momentum of V^0, and the superscript (+ or -) indicates the daughter particles.

Let Ψ be the rest reference system of V^0 with mass M (see *Fig. 7*). In this system we have:

$$M = \sqrt{p_{cm}^2 + m_1^2} + \sqrt{p_{cm}^2 + m_2^2}, \tag{2}$$

One can get

$$\begin{cases} p_{cm}^2 = \frac{1}{4M^2}(M^4 + m_1^4 + m_2^4 - 2M^2(m_1^2 + m_2^2) - 2m_1^2 m_2^2) \\ \alpha_{arm} = \frac{r_\alpha}{\beta}\cos\theta + \alpha_0 \end{cases} \tag{3}$$

where m_1 and m_2 are masses of daughter particles and $r_\alpha = \frac{2p_{cm}}{M}$, $\alpha_0 = \frac{m_1^2 - m_2^2}{M^2}$. Hence, considering $\beta \to 1$, we obtain the equation of an ellipse:

$$\frac{(\alpha - \alpha_0)^2}{r_\alpha^2} + \frac{p_T^2}{p_{cm}^2} = 1$$

For example, the Armenteros-Podolanski diagram for Ω and Ξ are shown in *Fig. 8*. Based on the obtained data, it is possible to determine the area on the diagram where we expect to observe Ξ and Ω.

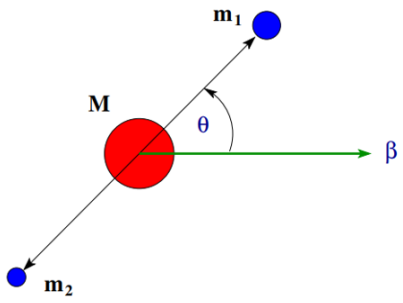

Figure 7: The rest reference system of V^0. θ is the angle between the direction of motion of the reference system and the direction of the momentum of one of the daughter particles.

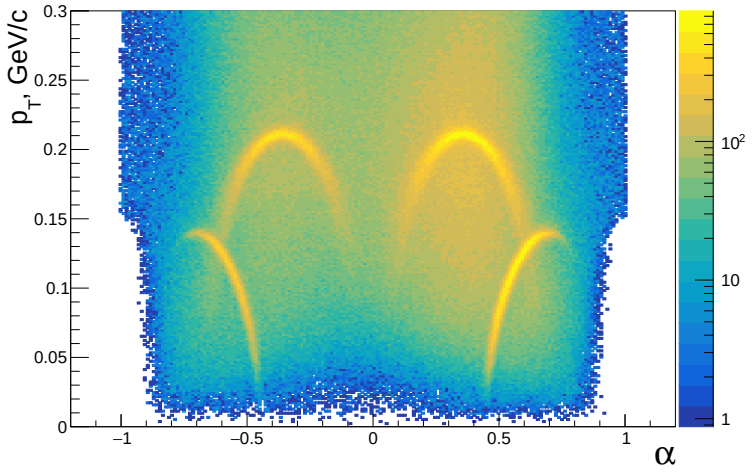

Figure 8: Armenteros-Podolanski diagram for Ξ and Ω.

4 Results

4.1 Invariant Mass Distributions

Fitting of invariant mass distributions was carried out using the function f:

$$f = N\left(\mu_1, \sigma_1^2\right) + N\left(\mu_2, \sigma_2^2\right) + P,$$

where $N\left(\mu_i, \sigma_i^2\right)$ is a normal distribution with parameters μ_i (mean value) and σ_i^2 (variance); $i = 1, 2$; P is a polynomial. The background was estimated via side-band method and substructed from initial invariant mass distribution. The regions

used for it are close to $[M_{PDG} - 6\sigma, M_{PDG} - 3\sigma]$ and $[M_{PDG} + 3\sigma, M_{PDG} + 6\sigma]$, the precise values depend on the p_T region and centrality. In *Fig. 9* and *Fig. 10*, the invariant mass distributions are shown, with errors representing statistical uncertainties.

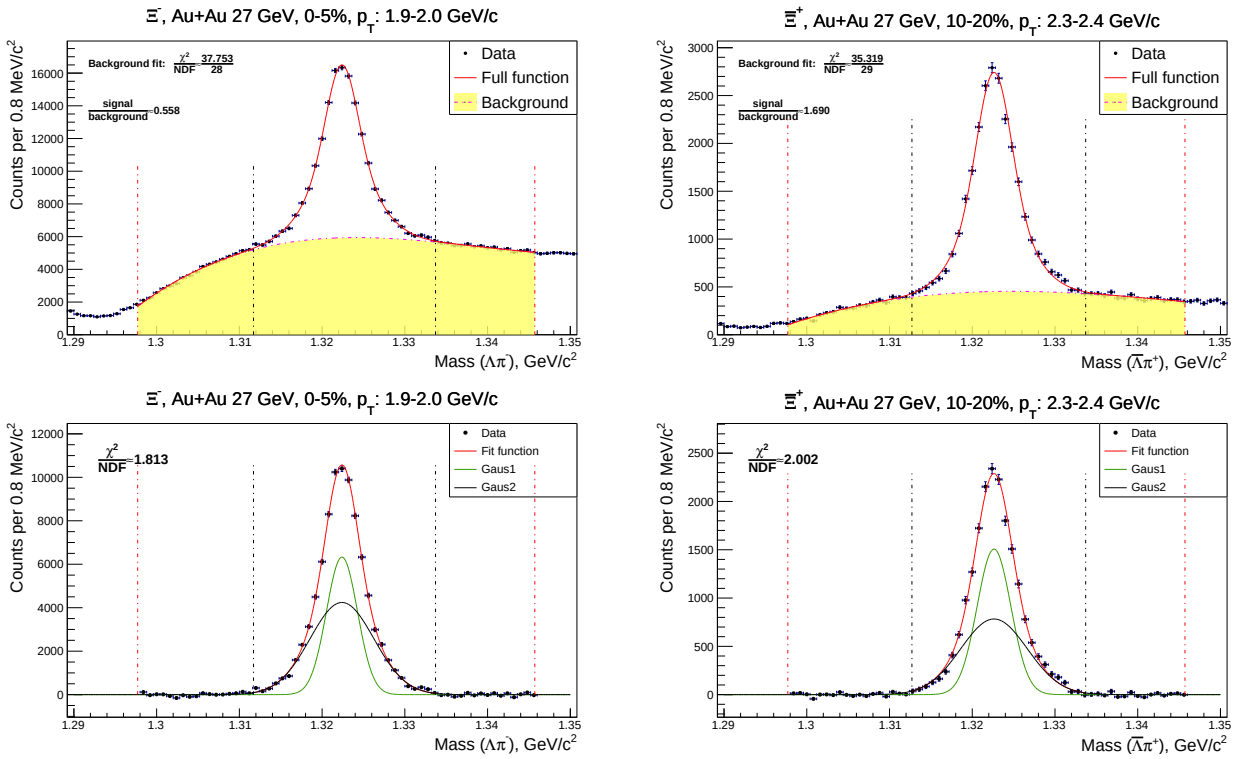

Figure 9: Invariant mass distributions of Ξ^- and $\bar{\Xi}^+$. The total distributions are shown on the top, the signals are shown on the bottom. The red solid line shows the fitting function, and the purple dashed line shows the background. The background was estimated via side-band method, the fit region is shown with vertical black and red dashed lines. The vertical black dashed lines shows both the signal peak fit and signal peak regions.

4.2 Spectra

In *Fig. 11* and *Fig. 12*, raw transverse momentum spectra for Ξ and Ω at different centralities are presented. The only spectra correction in this work was the decay mode probability correction.

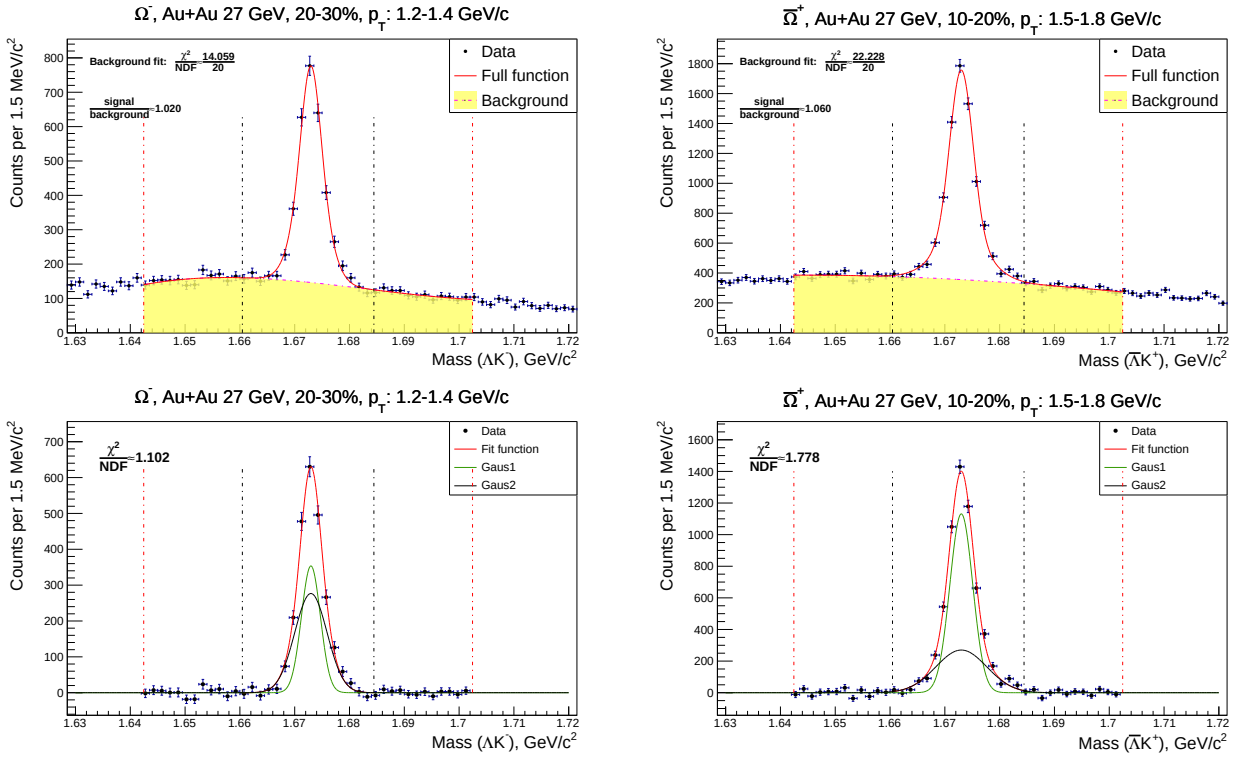

Figure 10: Invariant mass distributions of Ω^- and $\bar{\Omega}^+$. The fitting method and lines are depicted in *Fig. 9*.

At low values of transverse momentum, a suppression of particle yield is observed. This is primarily due to the unaccounted efficiency and acceptance of the detector in this region. At higher momentums spectra have exponential dependence, which is in consistency with the theory despite unaccounted detector efficiency because the it close to 1 in this p_T region.

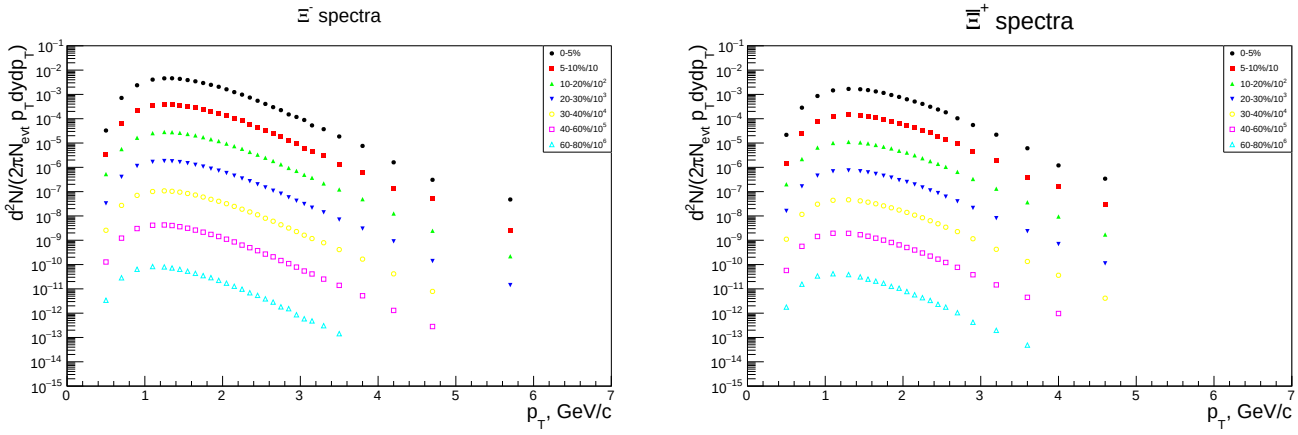

Figure 11: Transverse momentum spectra of Ξ^- and $\bar{\Xi}^+$ in the range of mid-rapidities ($|y| < 1$) . Vertical lines display statistical uncertainties.

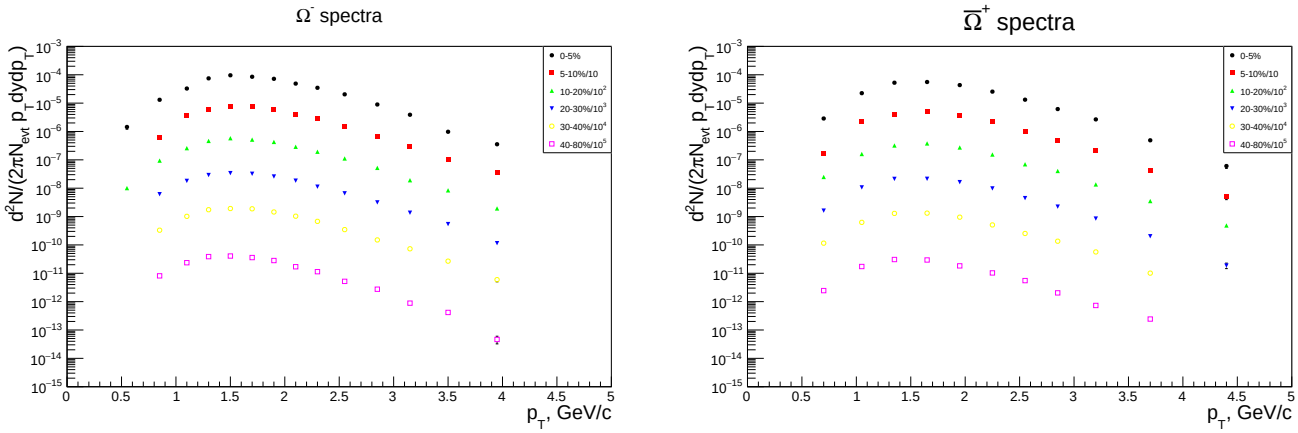

Figure 12: Transverse momentum spectra of Ω^- and $\bar{\Omega}^+$ in the range of mid-rapidities ($|y| < 1$). Vertical lines display statistical uncertainties.

5 Summary

In the this work, we were able to start studying quark gluon plasma using the strange hadrons produced in Au+Au collisions at 27 GeV energies with the *STAR* experiment. A number of results were obtained, the main ones being:

- The obtained invariant mass distributions match the tabulated values, demonstrating the correctness of this particle reconstruction method;
- The transverse momentum spectra in the area $p_T > 1.5$ GeV/c show an exponential dependence, which is in consistency with the theory.

CONCLUSION

The study of strange particle spectra is an important part of studying hot QCD matter. Further investigation of these particles will allow testing of theoretical predictions, thereby leading to a deeper understanding of the processes in high-energy and elementary particle physics.

References

[1] L. Adamczyk et al. (STAR Collaboration), Phys. Rev. Lett. 121, 032301 (2018).

[2] Adamczyk, L., Adkins, J. K., Agakishiev, G., Aggarwal, M. M., Ahammed, Z., Ajitanand, N. N., ... & Li, Y. (2017). Bulk properties of the medium produced in relativistic heavy-ion collisions from the beam energy scan program. Physical Review C, 96(4), 044904.

[3] K. H. Ackermann et al. (STAR Collaboration), Nucl. Instrum. Meth. A 499, 624 (2003).

[4] Podolanski, J., & Armenteros, R. (1954). III. Analysis of V-events. The London, Edinburgh, and Dublin Philosophical Magazine and Journal of Science, 45(360), 13-30